

Electrochemically cleanable pH electrode based on the electrodeposited iridium oxide-ruthenium oxide-titanium composite

Guangxing Hu^{a, b}, Yongxing Diao^{a, b}, Shuang Cui^{a, b}, Hongda Wang^{a, b, c}, Yan Shi^{a*}, Zhuang Li^{a, b*}

^a State Key Laboratory of Electroanalytical Chemistry, Changchun Institute of Applied Chemistry, Chinese Academy of Sciences, Changchun, Jilin, 130022, China

^b University of Science and Technology of China, Hefei, Anhui, 230026, China

^c Qingdao National Laboratory for Marine Science and Technology, Qingdao, 266200, China

E-mail: zli@ciac.ac.cn (Z.L.), sherry@ciac.ac.cn (Y.S.).

Electrochemical measurements of portable IOROE-based pH sensor and home-made Ag/AgCl electrode.

The stability of home-made Ag/AgCl electrode was assessed by immersing this electrode and commercial Ag/AgCl electrodes in 0.1 M KCl solution and using a CHI760e to test open-circuit potential for 8h. The potential changes of home-made Ag/AgCl electrodes in pH were assessed by immersing this electrode and commercial Ag/AgCl electrodes in a B-R buffer solution and adding a stoichiometric amount of 0.2 M NaOH solution. The selectivity of home-made Ag/AgCl electrode to common interfering ion (interference ion is 10^{-7} - 10^{-1} M Ca^{2+} , Na^+ , K^+ , Cl^- , NH_4^+ , Mg^{2+} , SO_4^{2-} , CO_3^{2-}) was assessed by placing home-made Ag/AgCl electrode and SCE in solutions (B-R buffer, pH=7) containing different concentrations of interfering ions and using a CHI760e to test open-circuit potential. The CHI760e and the small voltmeter were used to connect the sensors to compare the calibration of the pH sensor. Long-term deployment tests in natural water required portable IOROE-based pH meter and commercial glass pH meter to test for 14 days.

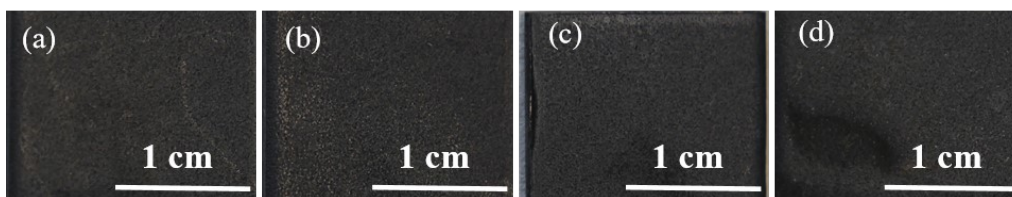


Figure S1. Effect of ruthenium-iridium concentration ratio in the plating solution on the coating. (a) $c(\text{Ir}^{3+}):c(\text{Ru}^{3+}) = 1:0$; (b) $c(\text{Ir}^{3+}):c(\text{Ru}^{3+}) = 1:1$; (c) $c(\text{Ir}^{3+}):c(\text{Ru}^{3+}) = 1:3$; (d) $c(\text{Ir}^{3+}):c(\text{Ru}^{3+}) = 1:5$.

The effect of varying iridium-ruthenium concentration ratios on the surface morphology of the electrode during electrodeposition is illustrated in Figure S1. The electrode surface exhibits a uniform black appearance and highest surface uniformity when the concentration ratio is 1:3. Conversely, when the concentration ratio deviates from 1:3, dot-like patterns are observed on the electrode surface. Therefore, we deduce that a concentration ratio of 1:3 is optimal for electrodepositing iridium-ruthenium composite materials in the plating solution.

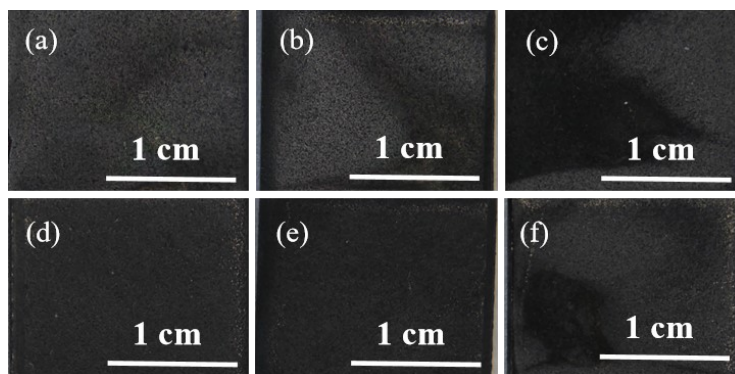


Figure S2. Effect of different in the plating solution on the coating. (a) pH = 2.00; (b) pH = 4.00; (c) pH = 6.00; (d) pH = 8.00; (e) pH = 10.00; (f) pH = 12.00.

Figure S2 demonstrates the impact of varying pH values on the surface morphology of iridium-ruthenium composite material during electrodeposition. A plating solution pH of 10.00 yields a uniformly black surface with the highest level of uniformity. Conversely, when the pH is 2.00 or 4.00, the surface of the electrode exhibits gray patches. Meanwhile, at pH 8.00 and 12.00, dotted patterns are observed on the electrode surface, resulting in a lower degree of surface uniformity. From these results, it can be concluded that the optimal pH value for the electrodeposition of the iridium-ruthenium composite material is 10.

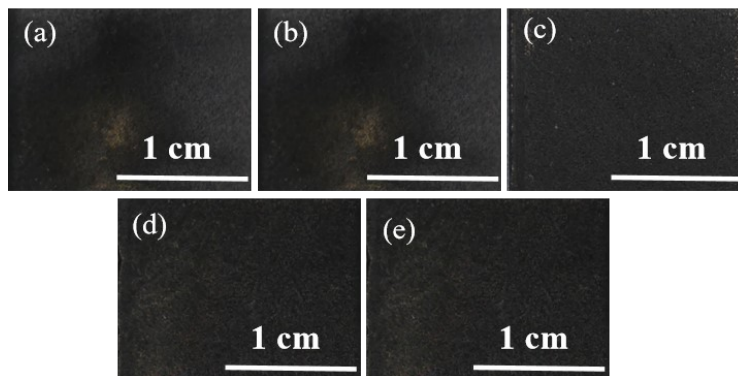


Figure S3. Effect of different concentrations of boric acid in the plating solution on the coating. (a) 0.1 M; (b) 0.2 M; (c) 0.3 M; (d) 0.4 M; (e) 0.5 M.

Figure S3 illustrates the effect of varying concentrations of boric acid on the surface morphology. At a concentration of 0.3 M, the electrode surface displays a consistent black appearance, indicating optimal coating uniformity. Conversely, when electrodeposition is performed using other concentrations of boric acid, the resulting coating exhibits gray patches and dotted patterns. From these results, we conclude that the electrodeposition of the iridium-ruthenium composite material is best achieved at a boric acid concentration of 0.3 M.

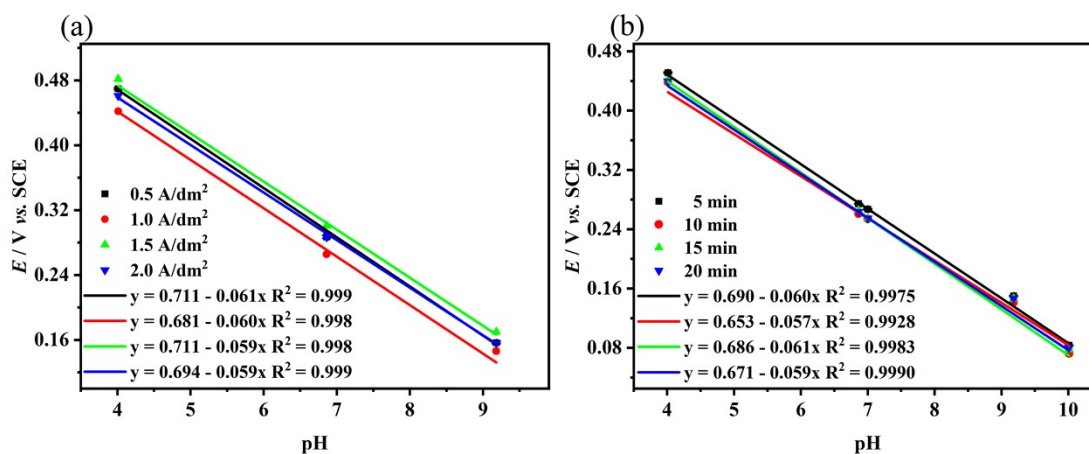


Figure S4. Effect of electrodeposition current density and electrodeposition time on pH response of EIRTE. (a) Current density; (b) Electrodeposition time.

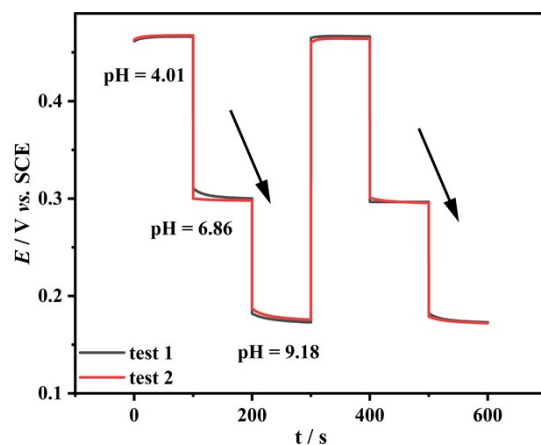


Figure S5. The hysteresis evaluation of IOROE by measure potential responses with an order of acid-alkali.

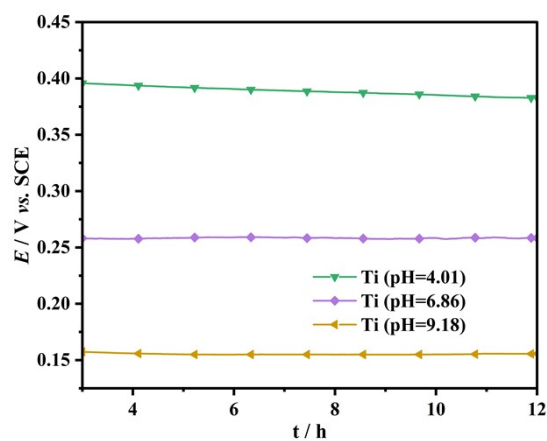


Figure S6. The potential responses of Ti for 12 hours at pH 4.01, 6.86 and 9.18. The electrode potential drops of Ti electrode were 19 mV (0.38 pH), 3 mV (0.06 pH), and 2 mV (0.04 pH) within 12 h in standard buffer solutions of pH 4.01, 6.86 and 9.18, respectively.

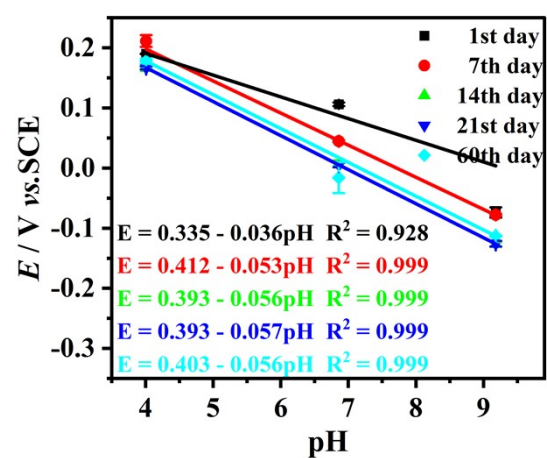


Figure S7. Calibration curves of commercial glass pH electrode during 60 days.

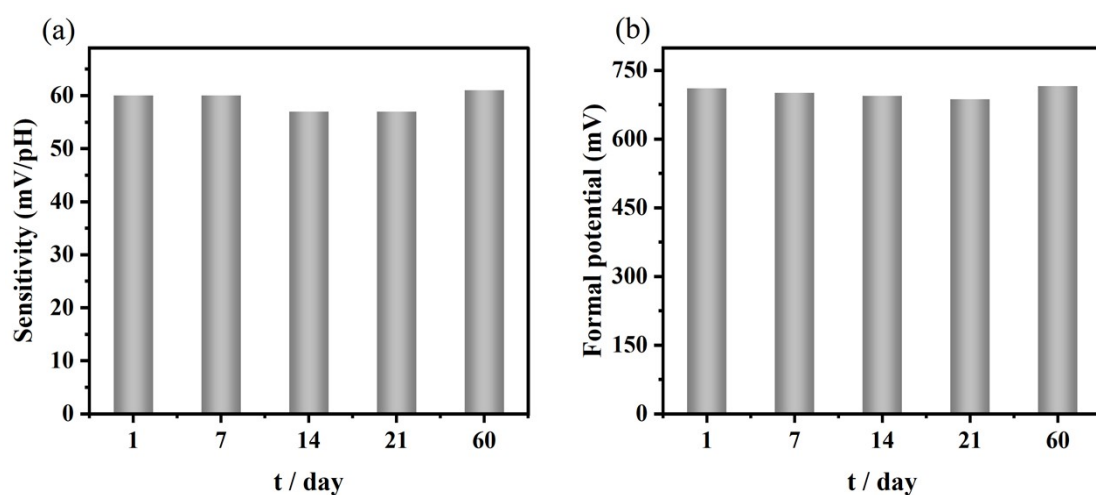


Figure S8. Sensitivity and formal potential changes of IOROE. (a) Sensitivity; (b) formal potential.

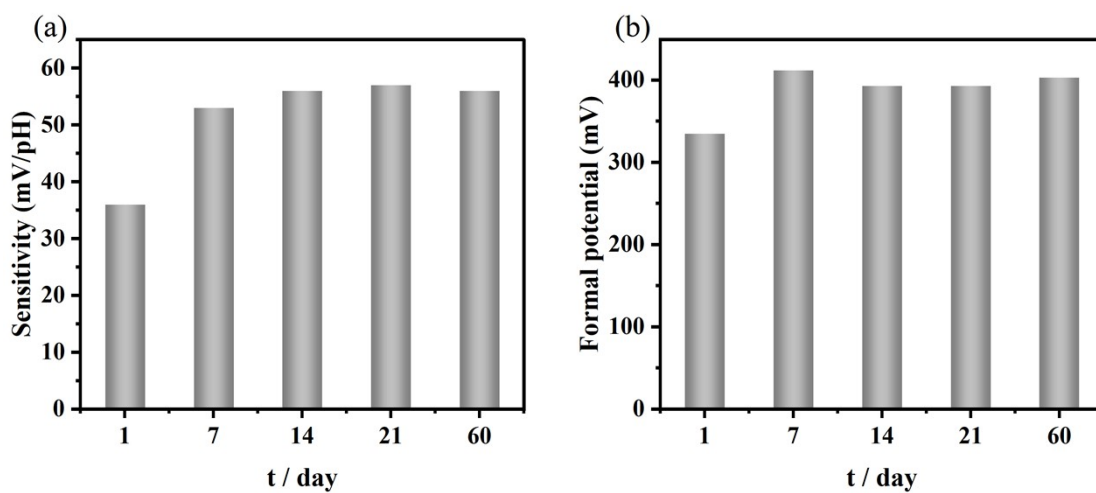


Figure S9. Sensitivity and situation potential changes of commercial glass pH electrode. (a) Sensitivity; (b) Situation potential.

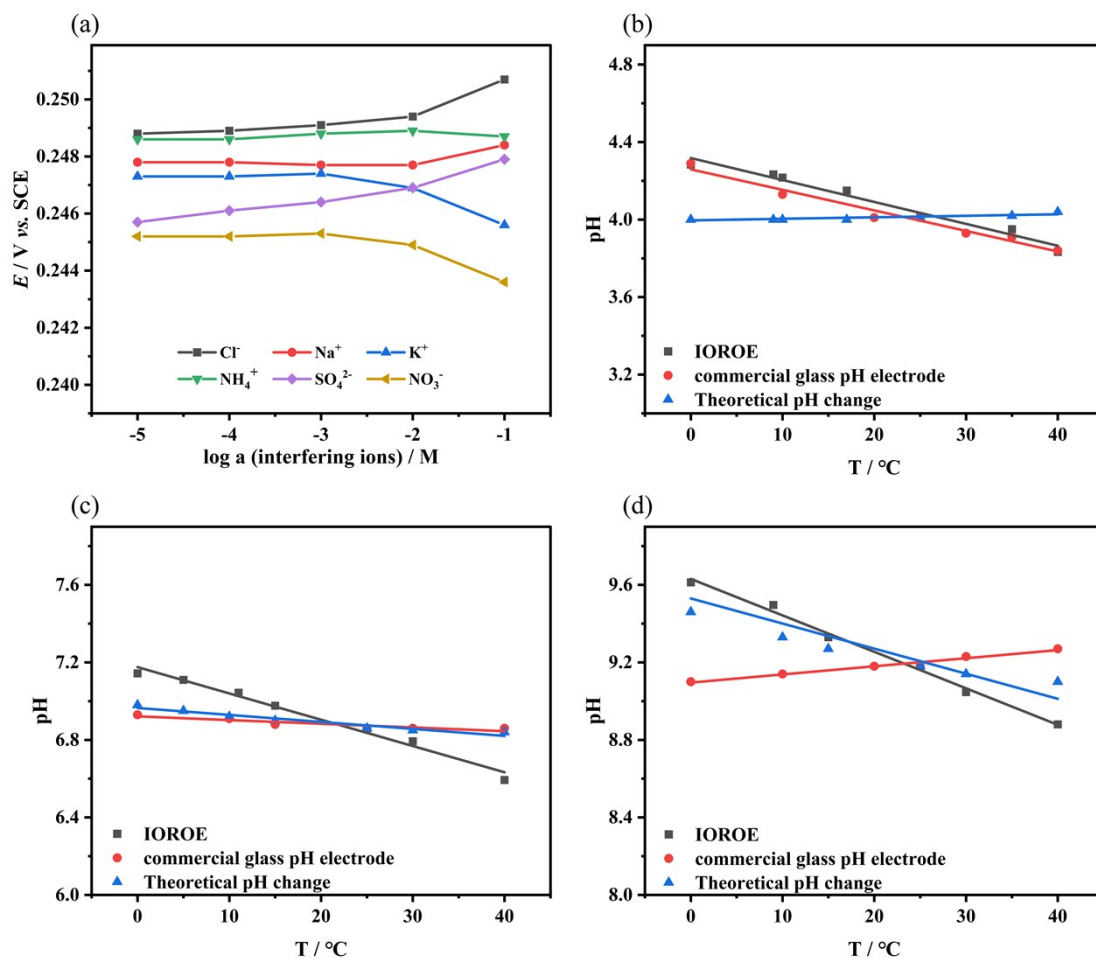


Figure S10. (a) The selectivity evaluation of IOROE by separation solution method and adjust the temperature from 0 to 40°C in (b) pH 4.01, (c) pH 6.86, and (d) pH 9.18.

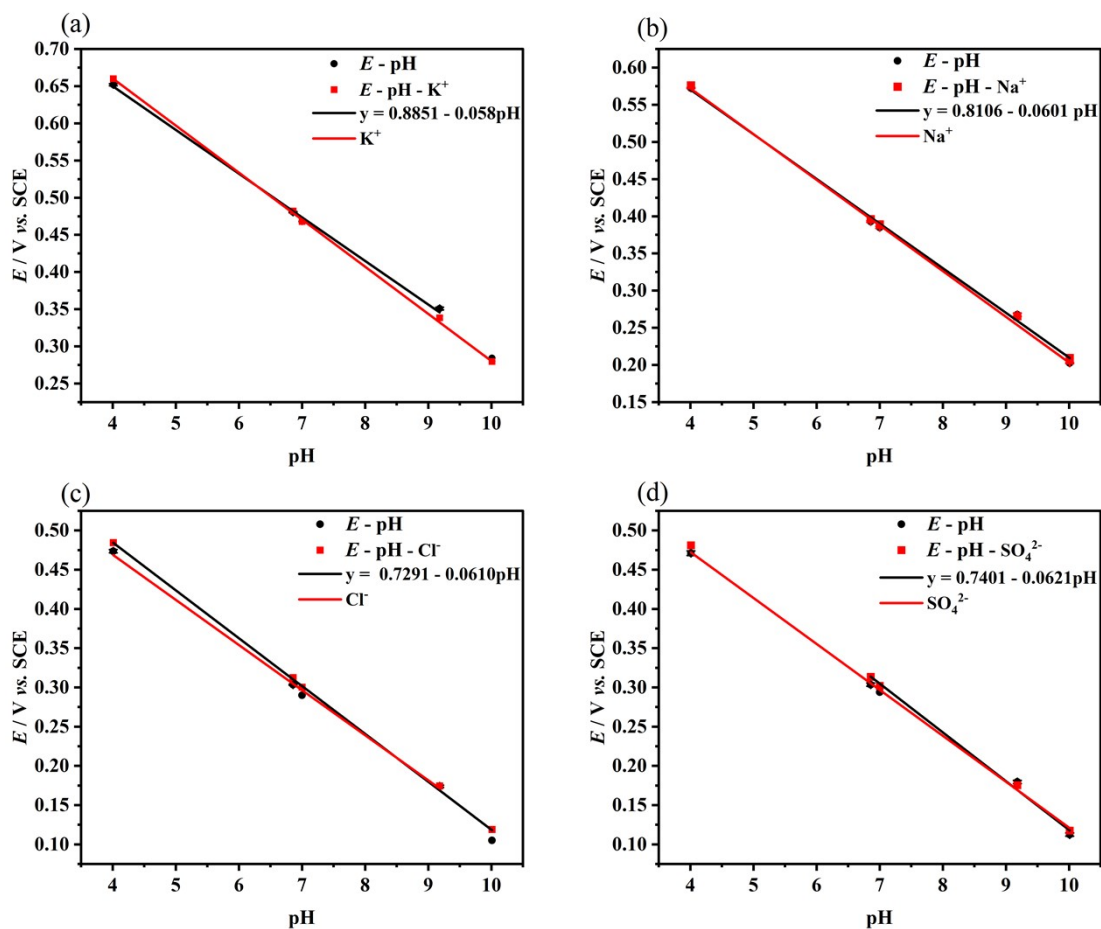


Figure S11. The selectivity of IOROE in the interfering ions. (a) K^+ ; (b) Na^+ ; (c) Cl^- ; (d) SO_4^{2-} . The standard buffer solution 1 mL containing the interfering ion ($0.1\text{ M } K^+$, Na^+ , Cl^- , and SO_4^{2-}) is added to the standard buffer solution volume 20 mL.

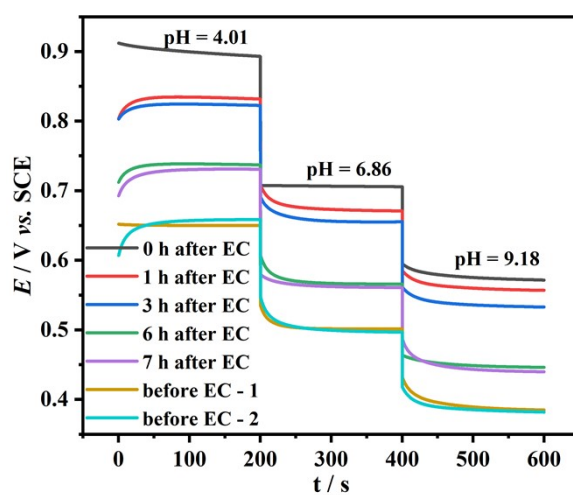


Figure S12. E-t curve of IOROE before and after EC in 4.01, 6.86 and 9.18.

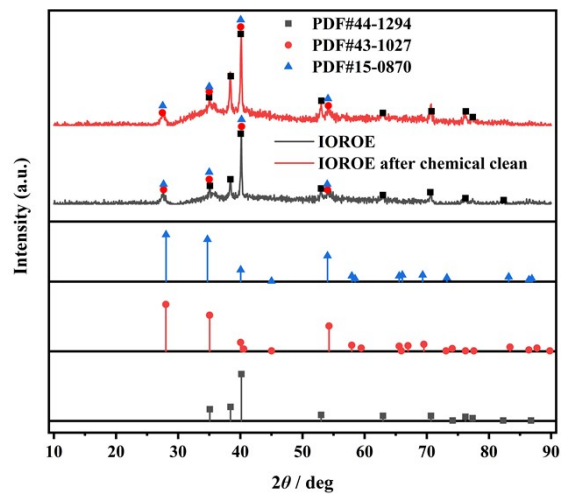


Figure S13. XRD of IOROE before and after EC.

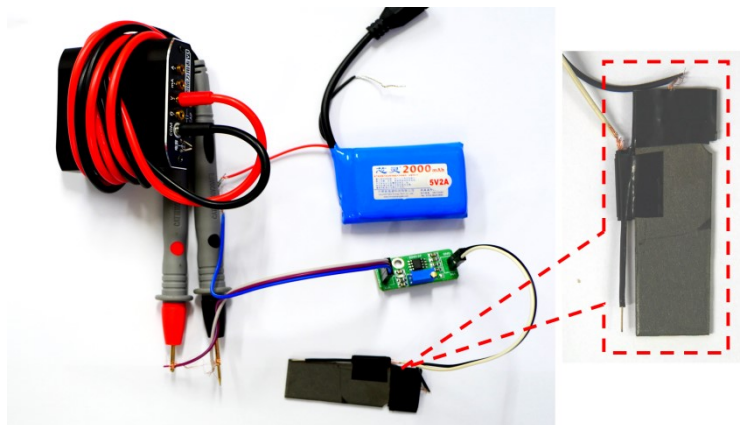


Figure S14. The structure of portable IOROE-based pH meter.

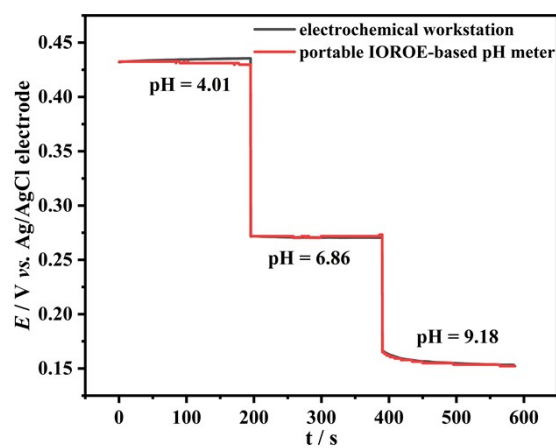


Figure S15. The potential response of IOROE-based pH sensor and electrochemical workstation in pH 4.01, 6.86, and 9.18.

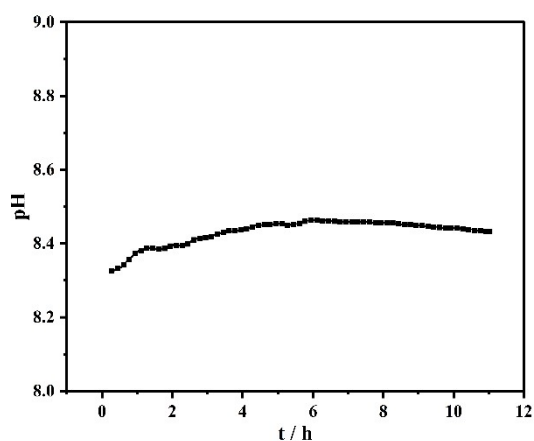


Figure S16. The stability of the portable IOROE-based pH meter in nature water.

Table S1. The IOROE sensitivity data sheet.

Test	1	2	3	average value	standard deviation
Sensitivity(mV/pH)	-0.0592	-0.0597	-0.0594	-0.0594	0.0003

Table S2. Summary of the sensing performance in iridium oxide, ruthenium oxide and in this work.

material	Detection range	Sensitivity / mV/pH	Response time / s
IrO ₂ nanowires ¹	2.5-13	90.1	
Ir/IrO ₂ ²	1.8-11.92	65.3	
TiO ₂ /IrO _x ³	1-13	69.9	
Pt/IrO _x ⁴	2-11	71.4	
IrO ₂ -RuO ₂ -Ti ⁵	2-12	50.8	4.0–13.5
RuO ₂ ⁶	4-10	58.1	2
This work (IOROE)	2-12	59.4	50

Table S3. Sensitivity data sheet for the different batch of IOROE.

electrode	1	2	3	average value	standard deviation
Sensitivity(mV/pH)	-0.0603	-0.0615	-0.0594	-0.0604	0.0011

- 1 L. Zhou, C. Cheng, X. Li, J. Ding, Q. Liu and B. Su, *Anal. Chem.*, 2020, **92**, 3844–3851.
- 2 Z. Zhou, D. Pan, C. Wang, H. Han, H. Wei and F. Pan, *J. Electrochem. Soc.*, 2021, **168**, 097501.
- 3 G. M. da Silva, S. G. Lemos, L. A. Pocrifka, P. D. Marreto, A. V. Rosario and E. C. Pereira, *Anal. Chim. Acta*, 2008, **616**, 36–41.
- 4 M. Zea, A. Moya, M. Fritsch, E. Ramon, R. Villa and G. Gabriel, *ACS Appl Mater Interfaces*, 2019, **11**, 15160–15169.
- 5 B. Liu and J. Zhang, *RSC Adv*, 2020, **10**, 25952–25957.
- 6 E. Tanumihardja, W. Olthuis and A. Van den Berg, *Sensors*, 2018, **18**, 2901.